Cislunar Orbit Determination and Tracking via Simulated Space-Based Measurements

Michael R. Thompson, Nathan P. Ré, Cameron Meek, Bradley Cheetham
Advanced Space, LLC

ABSTRACT

Building on previous work in cislunar orbit determination at Advanced Space, this paper demonstrates cislunar orbit determination via simulated optical measurements from another spacecraft in cislunar space. The goal of this work is to evaluate the potential performance (in terms of the uncertainties in the state of a target object) of space-based optical tracking filters in the vicinity of the Moon.

1. INTRODUCTION

As the Moon and cislunar space receive a renewed focus from both governments and commercial space companies, it is important to understand how well spacecraft and debris objects can be tracked in this volume. This is important from both a space domain awareness (SDA) standpoint for active satellites, and a safety-of-flight standpoint for uncontrolled objects. There are tens of thousands of trackable objects in Earth orbit compared to likely tens of objects in cislunar space, but Earth orbit is also a very sensor-rich environment. Nations and companies have spent decades building the infrastructure to track objects in orbit. This infrastructure does not exist for the cislunar domain, and in recent years, researchers and spacecraft operators have begun to approach passive methods such as optical tracking to address the problem of cislunar SSA. Estimating a spacecraft state via ground-based or space-based optical measurements up to GEO is a well-studied problem and is operationally performed by several companies and agencies. Space-based tracking in the cislunar domain is a more novel problem given challenges with low signal-to-noise ratio (SNR) observations, lunar exclusion angles, short data arcs, and nonlinear dynamics that stress basic assumptions and simplifications of most tracking filters. In this study, angular measurements are generated between two cislunar spacecraft, and random angular noise is added based on realistic values for optical sensors. These noisy measurements are processed in a sequential filter to refine the 6-dimensional state and covariance of the resident space object (RSO) over time.

This study demonstrates bounds on the potential performance of cislunar space-based surveillance systems from the standpoint of tracking filter design, trajectory design, and basic optical modeling. Given that any SSA modeling is dependent upon the optical characteristics of both the observing sensor and target spacecraft, this study seeks to be as optically agnostic as possible, and each examined case is performed with several "optical cutoffs" corresponding to different levels of observer sensitivity. While this work is not intended as a sensitivity study of target brightness or sensor sensitivity requirements, some insights are naturally provided in these areas as different optical cutoffs are explored.

The cislunar SSA/SDA field is still developing, and a number of previous studies have focused either on high-fidelity simulations of the apparent magnitude of cislunar objects, or on performing line-of-sight coverage analyses (including occultations and solar constraints) with potential observers and targets to inform constellation design. This study seeks to inform the field by simulating tracking with an operations-like filter and quantifying to what degree custody of targets can be maintained at multiple observer and target locations, and multiple optical cutoffs. Previous literature has shown that a multiple-observer constellation is typically required to maintain persistent SSA coverage of the cislunar domain through varied solar geometries of the lunar month. This work focuses on the tracking filter performance of a single observer tracking a single target, but the filter development and testing could be applied to a constellation-level tracking scheme in the future.

2. REVIEW OF GROUND-BASED CISLUNAR TRACKING

It is possible to monitor objects in cislunar space via ground-based assets with optical systems. A recent example of this was demonstrated during the *Chang'e 5* mission [1]. During this mission, which had very little publicly

available information regarding trajectories and real-time progress, sparse tracking via optical telescopes was possible [1]. Optical measurements gathered from the Pine Park Observatory in Colorado provided observations of *Chang'e 5* to a range of approximately 380,000 km, and the Numerica Telescope Network gathered observations at over 250,000 km [1]. A post-processing analysis based on the optical observations at Pine Park Observatory and the Numerica Telescope Network was able to reconstruct the outbound trajectory with a 3-sigma uncertainty on the order of 200 km in the radial direction and tens of km in the in-track and cross-track directions [1].

However, the return leg of the mission demonstrated some of the inherent limitations of an Earth-based optical tracking network. *Chang'e 5* returned to Earth with a very high solar phase angle and optical observations were mostly infeasible [1]. *Chang'e 5* is also a very large RSO compared to the numerous smaller satellites that will soon occupy the cislunar regime. These smaller targets will be much more stressing cases for ground-based optical networks.

Dao et al. simulated the visual magnitudes as seen from a ground observer using high-fidelity spacecraft models of both Galaxy-14, a large GEO communications satellite, and ANGELS, a smaller AFRL satellite, if they were in an Earth-Moon L_2 halo orbit [2]. The visual magnitude of Galaxy-14 varied from approximately 15 near full Moon to 22-23 near new Moon. Of note is that there were large gaps around both full and new Moon themselves due to lunar exclusion angles and the requirement of daylight observations respectively [2]. Near full Moon, the RSO is at its maximum brightness, but the Moon itself is as well, which can lead to sensor saturation. For the smaller ANGELS, the magnitudes varied from around 20 - 26 over the course of the lunar month [2].

Estimations by Ackermann et al. at Sandia National Laboratories have put the typical sensitivity of the Ground-Based Electro-Optical Deep Space Surveillance (GEODSS) network at a magnitude of around 18, and the experimental Space Surveillance Telescope (SST) at 19.5 [3]. For the visual magnitudes given by Dao et al., large satellites like Galaxy 14 would be visible to the Space Surveillance Network (SSN) for roughly 6 days out of every month near full Moon, and smaller satellites like ANGELS would never be visible.

The ability to see an RSO in cislunar space is a necessary, but not sufficient criteria for tracking it optically. There are a number of additional challenges, including short arcs that cannot fully characterize the state of a given RSO, a lack of viewing geometry diversity, and the inherent instability of many orbits in this regime (instability being a challenge because small maneuvers can yield large state changes) [4, 5].

The challenges associated with ground-based observations of targets near the Moon have led multiple analysts to examine the possibilities of utilizing space-based measurements for cislunar SSA, as described in the following section.

3. REVIEW OF SPACE-BASED CISLUNAR TRACKING CONCEPTS

This section will provide a brief overview of some space-based cislunar tracking concepts. It should be noted that this is an extremely large trade space, and it is difficult to provide truly "optimal" solutions. The performance of developed solutions will vary greatly based on the scale of the problem that is being addressed. Solutions can attempt to address the full "4π steradian" problem i.e. the space in all directions above the altitude of GEO, or they can be more tailored to specific regions, say the Earth-Moon L_1 and L_2 Lagrange points. The difference in scale between these two problems is immense both in the sheer volume that needs to monitored and in the number of observers that are likely necessary to fully cover the desired region.

Observers in more standard orbital regimes (LEO, GEO, etc.) where space-based SSA has been performed before can contribute to observations of cislunar objects. However, they suffer many of the same problems as ground-based observers - namely very large distances and prohibitive exclusion angles. Knister et al. found that outside of very high solar phase angles, LEO constellations could be utilized to provide some improvements over ground-based architectures, but still ultimately concluded that traditional orbital regimes and ground-based systems alone cannot provide consistent coverage, even with very large optical systems [6]. The paper recommended the evaluation of observers in non-traditional locations such as well above GEO, Lagrange points, or the lunar surface [6]. One such non-traditional location could be the High Orbits with Profound Eccentricity (HOPE) concepts by Cunio et al., which envision orbits with apogees multiple times higher than the altitude of GEO [7]. The orbits would be oriented out-of-plane such that near apogee, solar exclusions would be greatly decreased when observing the Earth-Moon L_1, L_2, or L_3 Lagrange points.

3.1 Lagrange Point Concepts

Vendl and Holzinger have studied families of periodic orbits at the Earth-Moon L_1 and L_2 points for monitoring the volume defined by a 20°frustum (a 20°cone with the "top" truncated by a plane at the limb of the Earth) from the surface of the Earth to the altitude of the L_2 Lagrange point [8]. The authors sought to identify Pareto-optimal periodic trajectories in terms of both observational capability and stability index of the observing spacecraft. A very important finding from this work was the takeaway that L_1 and L_2 Lyapunov orbits in a 1:1 synodic resonance, if properly phased, could provide near-continuous line-of-sight coverage to the volume of interest with desirable solar geometry. The utilization of a 1:1 synodic resonance can ensure that as the Moon orbits the Earth, the Sun is always roughly "behind" the observing spacecraft as it attempts to find RSOs within the target volume [8]. Note that in this work, the Lyapunov orbits with a 1:1 synodic resonance maximized the visibility within the volume of interest, but that does not necessarily mean that visibility at any one particular trajectory within that volume was optimized. As such, this is likely a very good solution for searching a large area of interest, but may not be the optimal solution for any one given trajectory.

Fowler et al. applied observability theory to the cislunar SSA problem for a number of observer and target trajectories [9]. The authors found that even with space-based observers, L_2 halo orbits in particular were difficult to observe based on both simple metrics (range, angular movement, unavailability) and empirical observability metrics.

3.2 Lunar Resonant Orbit Concepts

Frueh and Gupta et al. have investigated Earth-Moon 2:1 resonant orbits as orbits that provide favorable stability and observability properties for optical observations in cislunar space [10, 11]. They can be designed such that they have a periapsis near GEO and an apoapsis near that of the Moon. For the designs examined by the authors, the orbit precesses due to the gravitational influence of the Moon such that it traverses the entire orbital plane from GEO to the Moon over a period of 20 revolutions (10 lunar months). Bolden et al. studied a similar concept, a 3:1 lunar resonant trajectory, in conjunction with a number of other observers that could cue each other [4]. One of the key features of these orbits is that they can be very well-tracked via ground-based optical systems. A key consideration in any space-based tracking system is how well the state of the observing spacecraft can be known. Concepts that study observers at Lagrange point orbits can provide interesting viewing geometries, but operationally, there would likely be higher state uncertainties on these observers than observers in a more traditional orbit, and these observer errors would flow down to errors in the estimation of RSOs.

3.3 CHPS

The Air Force Research Laboratory Cislunar Highway Patrol System (CHPS) is an experiment to deploy space-based sensors near the Moon to test space-based surveillance technologies [5]. There is little publicly available information about the CHPS program, and it will not be discussed further in this paper.

4. MATHEMATICAL FRAMEWORKS

4.1 Trajectory Propagation

All propagation in this paper is performed in a full ephemeris model (i.e. without any assumptions of the circular restricted three body problem (CRTBP)). To translate orbits that may be perfectly periodic in the CRTBP into an ephemeris model, four patch points are taken from the CRTBP at apolune, perilune, and halfway between each in time. For each desired revolution of the trajectory these four patch points are placed into the ephemeris model based on the actual instantaneous positions of the Earth and Moon.

The trajectory is then iterated upon in a multi-shoot method such that a continuous trajectory with no maneuvers is achieved. This is a common method for generating continuous reference trajectories for cislunar orbits that may be perfectly periodic in the CRTBP, but obviously cannot be in a full ephemeris model [12, 13]. An example of this method can be seen in Figs. 1 and 2, which show the patch points and solved continuous trajectory respectively for a large L_2 halo orbit.

Truth trajectories for this analysis are propagated with gravitational fields of the Moon, Earth, Sun, and Jupiter, and a basic spherical SRP model.

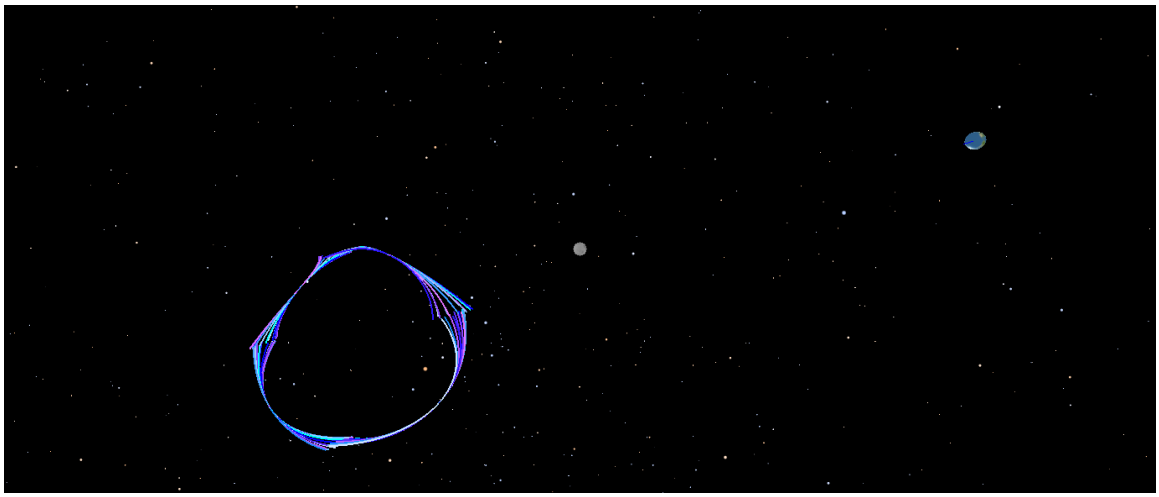

Fig. 1: Example L_2 halo orbit patch points from the CRTBP in the ephemeris model

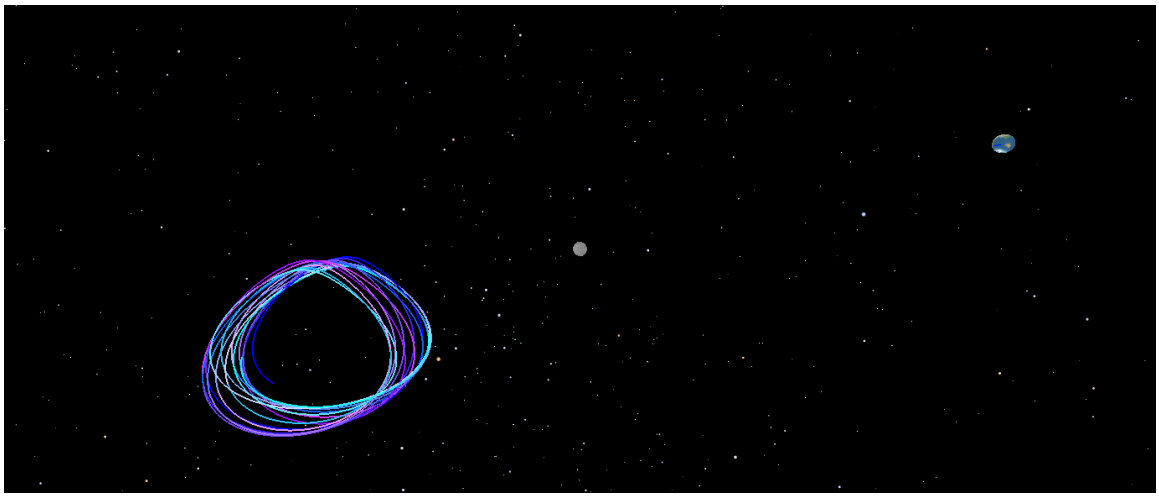

Fig. 2: Example L_2 halo orbit solved from patch points

4.2 Optical Modeling

The focus of this paper is primarily the ability to which angles-only measurements from space-based observers can maintain custody of RSOs in cislunar space. As such, the optical modeling is somewhat simplified.

The observed visual magnitude of an arbitrary RSO is modeled via one of the formulations of Hejduk which mixes diffuse and specular models [14]. Neither Earth-shine or Moon-shine are taken into account, although given the focus on RSOs in the vicinity of the Moon, Moon-shine could potentially provide a meaningful contribution, and should be examined in future work.

The visual magnitude equation is given in Equation 3, and the two contributing phase functions in Equations 1 and 2.

$$F_1(\varphi) = \frac{2}{3\pi^2}[(\pi - \varphi)\cos\varphi + \sin\varphi] \tag{1}$$

$$F_2(\varphi) = \frac{1}{4\pi} \tag{2}$$

$$M_v = -26.74 - 2.5\log(A\rho[\beta F_1(\varphi) + (1-\beta)F_2(\varphi)]) + 5\log(R) \tag{3}$$

In these equations, φ represents the solar phase angle, A is the cross-sectional area of the RSO, ρ is the albedo of the RSO, β is a mixing coefficient where 1.0 represents a fully diffuse RSO and 0.0 represents a fully specular RSO, and R is the range from observer to RSO.

4.3 Filter Dynamics

The navigation filter utilized for orbit determination in this analysis is a current epoch state U-D factorized covariance filter with backwards smoothing to a reference epoch. This is implemented in JPL's MONTE software, and is the baseline filter utilized for a number of JPL-navigated missions and cislunar navigation studies at Advanced Space [15, 16, 17]. Similar navigation setups utilizing this filtering framework have been developed in support of cislunar navigation studies for NASA's human spaceflight program and the upcoming CAPSTONE mission [18, 19, 17].

The filter utilized for this analysis estimates the state of the target RSO and a scale factor to the solar radiation pressure calculated by the baseline model. The baseline SRP model for this case is a basic spherical model. There are additionally stochastic accelerations re-estimated at a batch time of 1 hour. Less frequent batch times that are more typical of interplanetary radiometric navigation (8 hours, 12 hours, etc.) were experimented with before this shorter batch time was chosen. Less frequent batch times are feasible for some cislunar SSA setups, but not all.

Table 1: SSA filter estimated parameters

Parameter	Notes
State	
SRP	Estimated as a scale factor relative to the baseline model
Stochastic Accelerations	Re-estimated at a 1 hour batch time

In this analysis, only the properties of the target RSO are estimated; however, the filter has the capability to simultaneously estimate the state of the target RSO and the observer spacecraft. Hill, Born, Parker, and several other authors have shown that the cislunar environment, particularly near the Earth-Moon L_1 and L_2 points, has some key features in dynamical systems theory that can allow for the co-estimation of both relative and absolute states of two cooperating spacecraft with radiometric measurements between them [20, 21]. In the context of SSA, it obviously cannot be assumed that any two spacecraft are cooperative, but optical measurements in the cislunar environment could provide the necessary information for co-estimating the states of multiple spacecraft and could lead to a future where autonomous navigation coupled with cislunar SSA is possible.

5. FILTER PERFORMANCE

5.1 Setup and Constraints

The optical modeling setup was previous discussed in Section 4.2. For all analysis below, the same RSO properties are utilized to allow for easy comparisons between cases. The optical properties of the target RSO are given in Table 2. The size of this hypothetical RSO is larger than a CubeSat-class spacecraft, and is meant to be representative of a medium-sized satellite that could operate in cislunar space with enough propulsion capability to potentially perform large maneuvers - in short, a class of spacecraft that should be well-tracked for SDA or safety-of-flight concerns.

Table 2: RSO optical properties

Property	Value
Area	13.89 m^2
ρ	0.17
β	0.9

Angles-only measurements are generated at a fixed time step with a fixed Gaussian error. The angular noise value is based on the Canadian *Sapphire* satellite, a rare example of a space-based optical payload with some open-source publications summarizing its on-orbit performance [22, 23, 24]. The integration time required for optical measurements is

obviously a function of the specific observer optical equipment and noise environment, but to ensure that this analysis was sensor-agnostic, a generic value was chosen. It was set to a somewhat high integration time given some of the known challenges in cislunar SSA (low SNR, slow angular motion, short arcs, etc.).

Solar, lunar, and Earth exclusion angles are also very hardware-dependent and can be somewhat mitigated via sunshields or other technologies. The exclusion angles utilized for this analysis are informed by Vallado et al., which provided generic values for both solar and lunar exclusion angles [25]. For this analysis, an Earth exclusion angle constraint is set to be equal to the lunar constraint utilised in Vallado's analysis. The measurement simulation parameters and constraints are given in Table 3. In the analysis below, the limiting magnitude of observers is varied to study the effect on the filter solutions.

Note that all of these parameters can be easily changed in the simulation setup to tailor this analysis for a particular desired RSO or particular set of optical capabilities.

Table 3: Simulated angular measurement properties and constraints

Property	**Value**
Measurement Cadence	5 min
Angular Noise (1-sigma)	6 arcsec
Solar Exclusion Angle	30 deg
Lunar Exclusion Angle	10 deg
Earth Exclusion Angle	10 deg
Target Illuminated	True
Target Occulted	False
Visible Magnitude	Varied

The trajectories utilized in this analysis are given in Table 4, and a plot is provided in Fig. 3. There are four trajectories from families of periodic orbits in the CRTBP, and one trajectory that is a more typical Moon-centered orbit.

There are two L_2 halo orbits - one close to the Moon with a large out-of-plane amplitude and one with much less out-of-plane motion, and further away from the Moon. There is an L_2 Lyapunov orbit in a 1:1 synodic resonance with the orbit of the Moon. This orbit exists in the Moon's orbital plane about the Earth, and due to the synodic phasing, the solar phase angle remians similar for the entire month. Taking inspiration from the work of Vendl and Holzinger, if properly phased, this can provide continuous desirable solar geometry in the vicinity of L_2 and no solar exclusions [8]. There is a Near Rectilinear Halo Orbit (NRHO), which will be home to the future Lunar Gateway and the upcoming CAPSTONE mission. And finally, there is a lunar frozen orbit, which is a large, highly eccentric Moon-centered orbit. In the analysis below, each of these will be further expanded upon.

Table 4: Target and observer orbital parameters

Spacecraft	**Period**	**Max Z Amplitude**
L_2 Halo (Distant)	14.77 days	-13,019.3 km
L_2 Halo (Close)	12.74 days	70,540.8 km
L_2 Lyapunov	29.54 days	0 km
NRHO	6.56 days	-69,792.4 km

Spacecraft	**SMA**	**Inclination**	**Eccentricity**
Lunar Frozen	6,207 km	57 deg	0.67

There is a particular focus on tracking RSOs in the Earth-Moon L_2 vicinity for multiple reasons:

- They are particularly difficult to track via ground-based sensors due to persistent lunar exclusion zones.
- The vicinity is already occupied with one spacecraft, and there are multiple planned missions that will soon join it.
- Space-based sensors struggle to observe the L_2 vicinity more so than other cislunar regions [9].

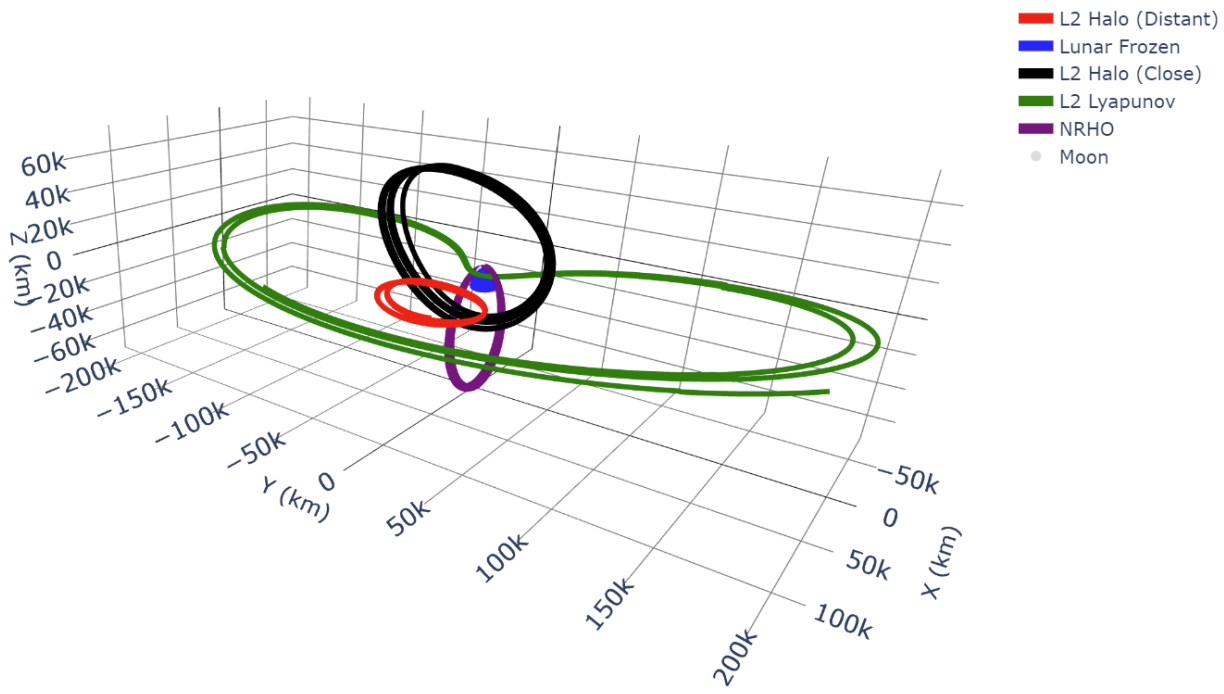

Fig. 3: Analyzed trajectories in a Moon-centered Earth-Moon rotating frame

This analysis focuses on RSOs at libration point orbits or at the Moon. As discussed in Section 3, there is a *major* difference in scale between this problem, and the full "4π steradian" problem. Future analysis should be performed to determine the degree to which observers can maintain custody of RSOs in high altitude regions away from the Moon.

5.2 L_2 Halo (Distant) RSO, NRHO Observer

The first case examined is the case of an observer in an NRHO and an RSO in a distant L_2 halo orbit. The NRHO is of particular interest due to the upcoming missions that will be utilizing it. NASA's Lunar Gateway is being designed to operate in a 9:2 lunar resonant NRHO, and could potentially host external payloads such as optical telescopes in the future. Additionally, the upcoming CAPSTONE mission, which is designed to be a pathfinder for navigation operations and technologies in the NRHO, is scheduled for an upcoming launch and does have a small optical payload onboard that could be utilized for experiments [26].

The simulated visual magnitude of an RSO in a distant L_2 halo orbit as seen by an observer in an NRHO over a period of 6 months is shown in Fig. 5. There are periodic trends in the visual magnitude, primarily driven by the motion of the observer spacecraft in the NRHO. This NRHO travels from within 2,000 km of the Moon to nearly 70,000 km away from the Moon in the out-of-plane direction. This leads to large fluctuations in the range between the observer and the RSO, hence the fluctuations in the visual magnitude. In addition to the fluctuations caused by changes in the range, there are periodic trends caused by the precession of the solar phase angle over the course of the lunar month. This is to be expected, and is a well-understood trend.

The setup of an NRHO observer and L_2 halo RSO does not need to contend with Earth or lunar exclusion events, but does occasionally need to contend with Solar exclusions, depending on the phasing. However, this analysis made no attempt to phase the orbit such that solar exclusion events were avoided. The reference NRHO utilized by Lunar Gateway is phased such that no Earth eclipses occur, and a similar strategy could potentially be followed in the design of a dedicated SSA asset to avoid solar exclusions in the NRHO [27].

In exploring the filter performance of angles-only measurements, the problem was found to be very sensitive. This was not necessarily surprising as both the observer and RSO are in three-body orbits that stress some of the baseline assumptions of navigation filters. The authors found that long data arcs were generally not possible, as the filter would eventually diverge. An example of such divergence is shown in Fig. 6.

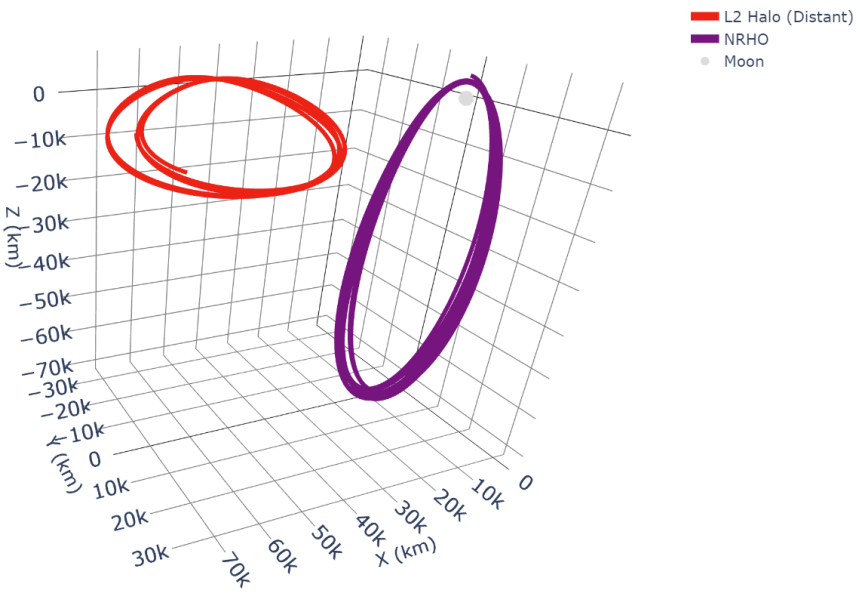

Fig. 4: 3D view of the NRHO observer and distant L_2 halo RSO in a Moon-centered Earth-Moon rotating frame

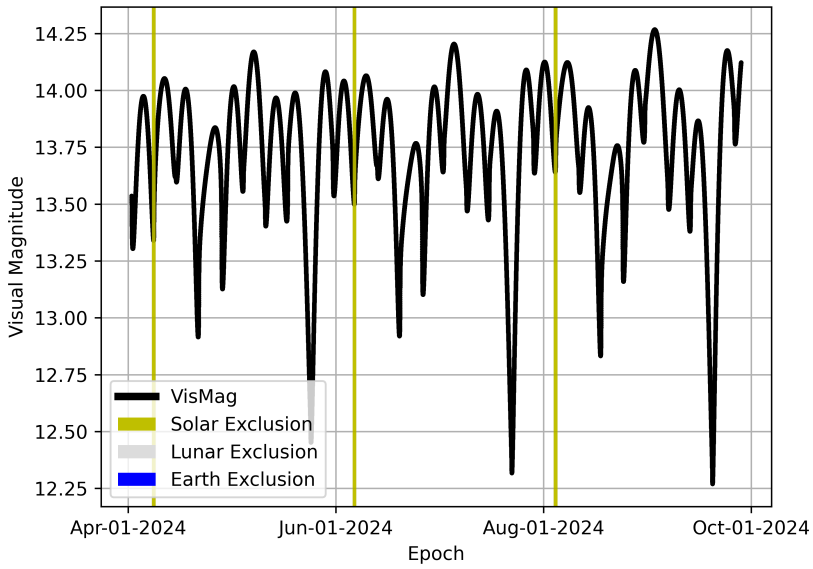

Fig. 5: Simulated visual magnitude of a distant L_2 halo RSO from an NRHO observer

In this case, the estimated trajectory departed from the truth trajectory and never recovered. Similar results were seen by Greaves and Scheeres when attempting to track an NRHO via angles-only measurements as it passed through perilune [28]. Note that in this case, the divergence was not associated with an NRHO perilune, but rather consistently occurred once the RSO had performed approximately 1.5 revolutions (around 21 days).

Despite this eventual divergence, with short data arcs on the order of 1 - 1.5 revolutions of the RSO, the angles-only measurements as gathered from the NRHO were able to estimate the state of the L_2 halo orbit. Three-sigma results for three different theoretical limiting magnitudes are provided in Fig. 7.

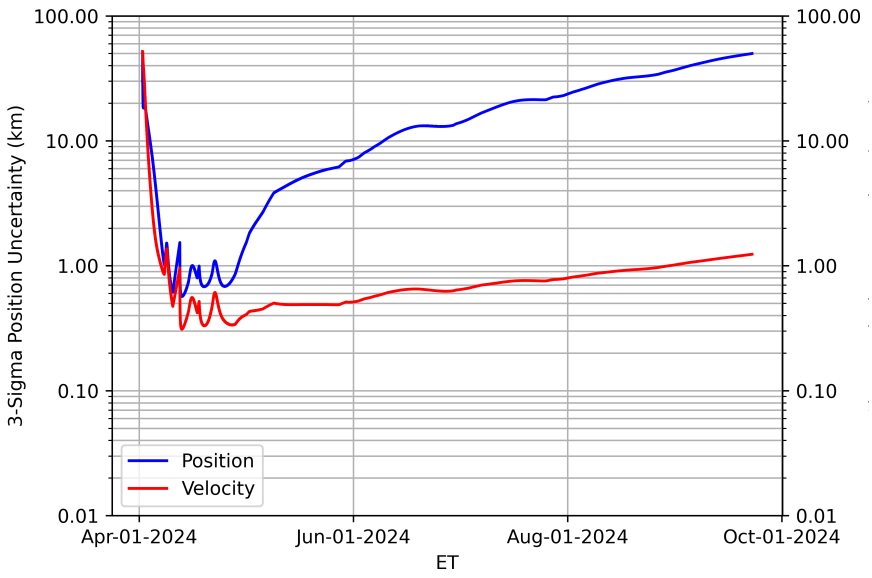

Fig. 6: An example of filter divergence with an NRHO observer and L_2 halo RSO (3-sigma, km for position, cm/s for velocity)

Note that in this case, even with the most capable optical sensor, it took approximately 1 week for the solution to converge to a steady-state value where the uncertainty plateaus. This is a key difference between orbit determination in the Earth environment and orbit determination in the cislunar domain. For objects in Earth orbit, an OD solution can be well-refined with relatively little data - a handful of optical observations or radar passes. This is not the case for cislunar orbits. Optical measurements must be spread across a reasonable fraction of the orbit (roughly half for this particular halo orbit) before the estimate approaches a steady-state value.

For the most capable optical cutoff (M = 14), the angles-only measurements were able to maintain custody of an RSO in an L_2 halo orbit with a 3-sigma uncertainty of 1-2 km in position and less than 1 cm/s in velocity. Less capable optical sensors suffered additional outages due to their limiting magnitude, but could still provide solutions with the same order of magnitude of errors during time periods where measurements are being gathered.

For the monitoring of active, potentially maneuvering spacecraft, near-continuous coverage is likely required, but for tracking defunct objects or debris, it may be acceptable to allow gaps of multiple days at a time, after which the RSO could be easily re-acquired depending on the stability of the orbit.

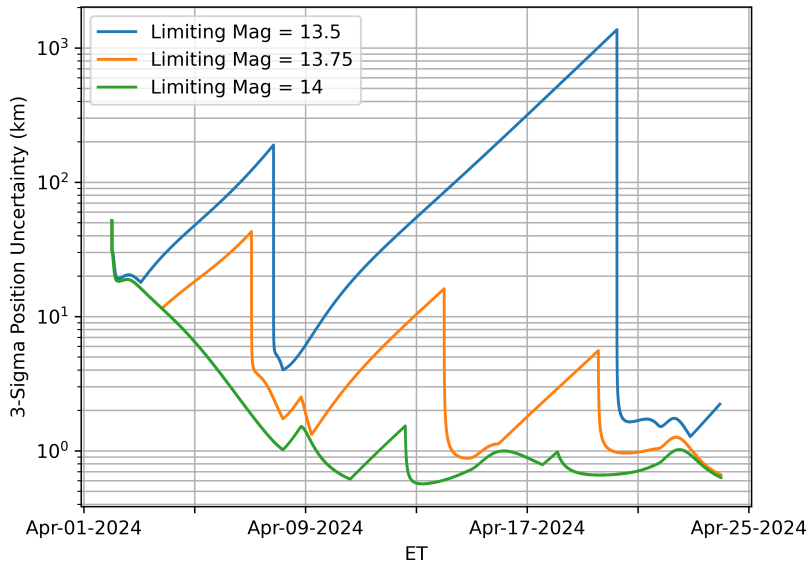

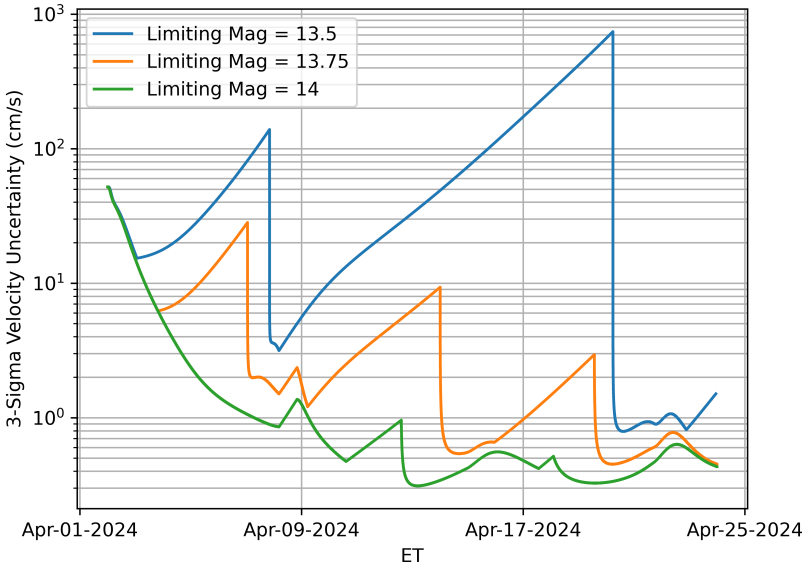

Fig. 7: 3-sigma covariances on the state estimation of a distant L_2 halo RSO from an NRHO observer

5.3 L_2 Halo (Distant) RSO, L_2 Halo (Close) Observer

The next case examined is the case of one spacecraft in an L_2 halo orbit observing another. The RSO is the same trajectory as studied before, the "L_2 Halo (Distant)" spacecraft. The observer spacecraft in this case is closer to the target RSO on average than an observer in an NRHO. Much like the NRHO, this particular L_2 halo provides opportunities for dual uses. The observer orbit provides a continuous view of Earth, and near-continuous coverage of the lunar far side with a focus on northern latitudes.

The simulated visual magnitude of the given RSO as seen by an observer in the given L_2 halo over a period of 6 months is shown in Fig. 9. Many of the same trends that were present for the NRHO observer case are once again present.

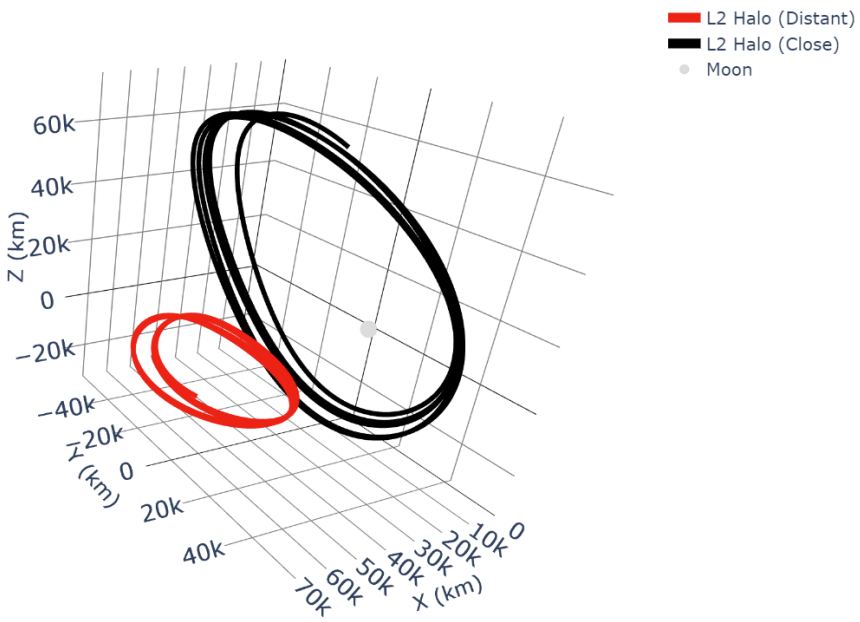

Fig. 8: 3D view of the close L_2 halo observer and distant L_2 halo RSO in a Moon-centered Earth-Moon rotating frame

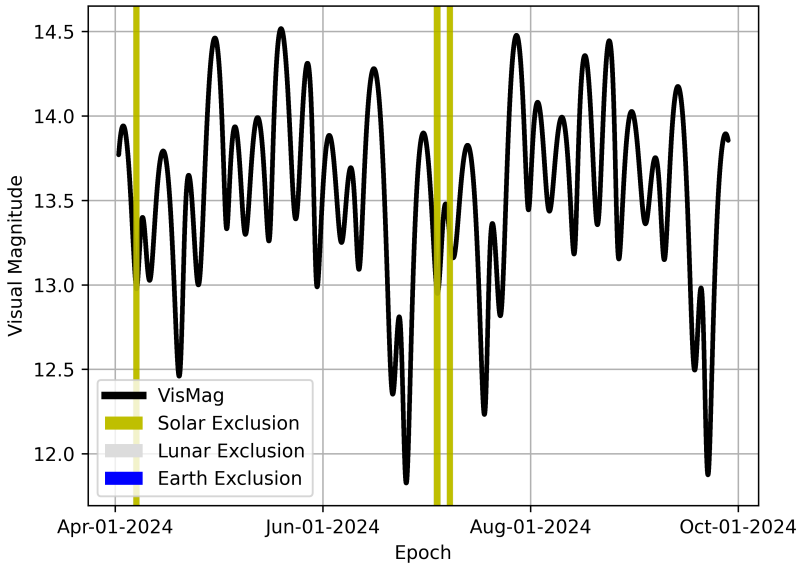

Fig. 9: Simulated visual magnitude of a distant L_2 halo RSO from another L_2 halo observer

There are occasional solar exclusion events, but no Earth or Moon exclusions. On average, the RSO is slightly brighter over time when compared to the case with an NRHO observer due to the closer range.

In estimating the state based on angular measurements, the filter would once again diverge with a data arc longer than around 21 days. Using a 21 day data arc, the resulting solution covariances are shown in Fig. 10.

For a limiting magnitude of 14, once a solution reached steady-state, the state of the RSO could be estimated with a 3-sigma uncertainty of 400-500 meters in position and less than 1 cm/s in velocity. These are results that are on the

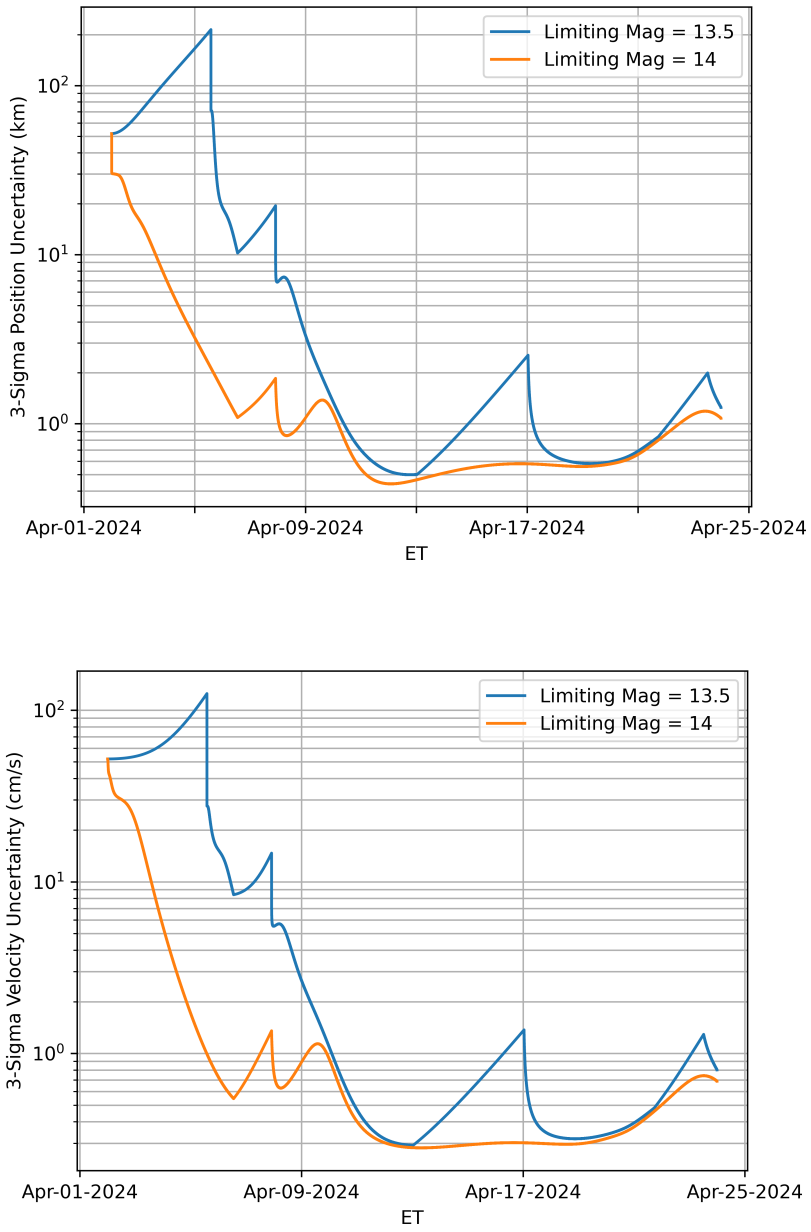

Fig. 10: 3-sigma covariances on the state estimation of a distant L_2 halo RSO from another L_2 halo observer

same order of magnitude as the results seen by the NRHO observer. For a slightly less capable sensor with a limiting magnitude of 13.5, there are outages where the 3-sigma position covariance rises to tens of kilometers. As discussed in the previous section, this could be acceptable depending on the application and what object is being tracked.

5.4 L_2 Halo (Distant) RSO, L_2 Lyapunov Observer

Based on the work of Vendl and Holzinger, L_1 and L_2 Lyapunov orbits with synodic resonances can provide pareto-optimal trajectories for observing the large volume of space between Earth and the Moon [8]. They are relatively stable compared to other three-body libration point orbits, and, if properly phased, can view large portions of the volume along the Earth-Moon line at a low solar phase angle. For a Lyapunov trajectory exactly in a 1:1 synodic resonance, the observer will traverse its periodic orbit at the same rate that the Sun appears to rotate about the frame. If the observer starts at a low solar phase angle, this angle will remain low.

Such an example is simulated for this case. An L_2 Lyapunov orbit with a 1:1 synodic resonance is phased such that it starts at a local minimum of the solar phase angle while attempting to observe the same distant L_2 halo studied previously. The simulated visual magnitude and exclusion constraints are shown in Fig. 12.

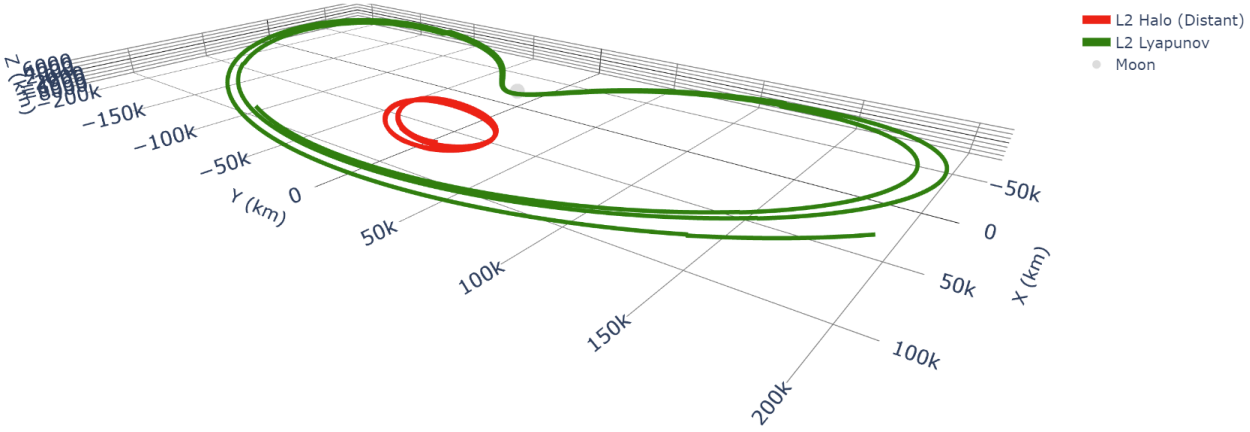

Fig. 11: 3D view of the L_2 Lyapunov observer and distant L_2 halo RSO in a Moon-centered Earth-Moon rotating frame

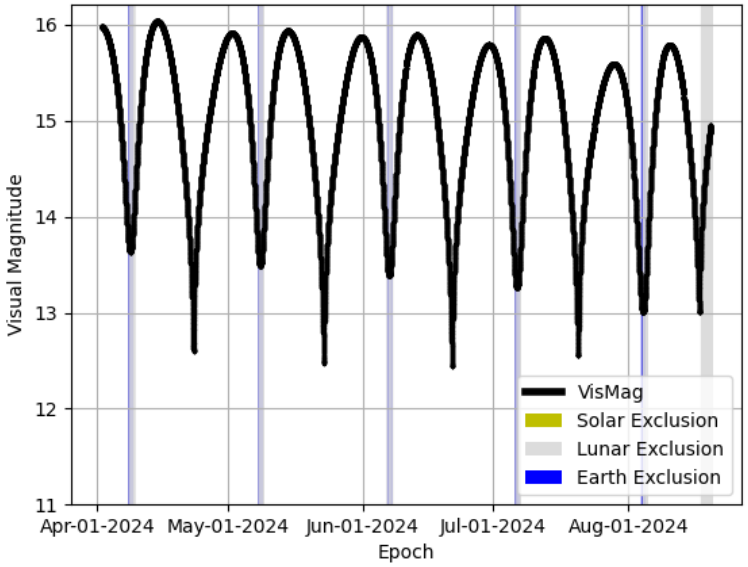

Fig. 12: Simulated visual magnitude of a distant L_2 halo RSO from a 1:1 synodic resonant L_2 Lyapunov observer

Due to the 1:1 synodic resonance, there are no solar exclusions, but there are monthly Earth/lunar exclusions as the

observer passes over the Earth-Moon line and looks back towards L_2. The solar phase angle stays low for the entire orbit, so the fluctuations in the simulated visual magnitude are driven primarily by the range from the observer to the RSO. Of note here is that the fluctuations in visual magnitude are quite large. For the first two examples of observers in an NRHO and another L_2 halo observing the distant L_2 halo RSO, the visual magnitude varied from 12 - 14.5. For the Lyapunov orbit observer, the magnitude fluctuates from 12.5 - 16.

The cause is, of course, that the 1:1 L_2 Lyapunov is a very large trajectory. Over a single synodic month, the observer will lead the Moon by 200,000 km, trail it by the same magnitude, travel 130,000 km beyond the Moon's orbit (with respect to the Earth), and flyby the Moon at an altitude of less than 3,000 km. The furthest points in this orbit are very far away when compared to the distances that an NRHO or L_2 halo observer must contend with if tracking an RSO near L_2. In short, the tradeoff for gaining the solar geometry advantage of a 1:1 Lyapunov trajectory are the large distances that the observer must handle. When evaluated in a filter for limiting magnitudes of 15 and 16, the covariances of the estimated trajectory are given in Fig 13.

With the exception of the Earth/lunar exclusion angle constraint, a limiting magnitude of 16 can maintain persistent coverage of the desired RSO. The observer with a limiting magnitude of 15 cannot, and can only make observations for two periods in each orbit. As seen in the previous two cases, the filter diverges after approximately 21 days. One of the expected benefits of the L_2 Lyapunov orbit was the fact that it circumnavigates L_2, providing opportunities to observe the target RSO from every direction in the XY plane. The hope was that this could decrease the uncertainty compared to the L_2 halo observers, but the benefit was not fully realized, potentially due to the 21 day data arc.

The case with a limiting magnitude of 16 still maintains relatively good custody of the RSO, with 3-sigma covariances of 2-3 km in position and 1-2 cm/s in velocity.

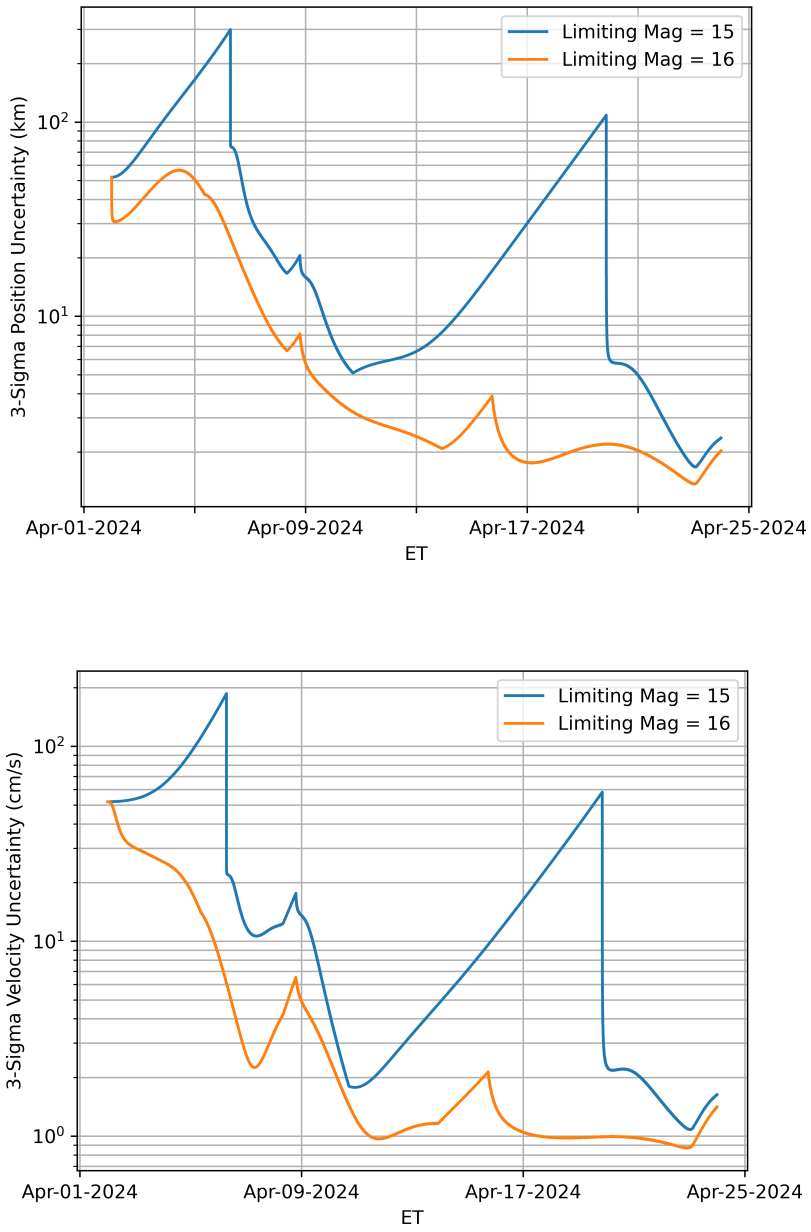

Fig. 13: 3-sigma covariances on the state estimation of a distant L_2 halo RSO from a 1:1 synodic resonant L_2 Lyapunov observer

5.5 Lunar Orbit RSO, L_2 Halo (Close) Observer

The final case examined studies the problem of an observer in a libration point orbit, but an RSO in a more typical lunar orbit. Orbits at the Moon are usually quite unstable unless they are at low altitudes. This case examines a "frozen" lunar orbit, a category of larger lunar orbits which exhibit quasi-stable behavior over time [29, 30]. Such orbits have been proposed for communications relays for future lunar networks, including the next-generation communications relay for the China National Space Administration (CNSA) lunar program, set to launch with or near *Chang'e 7* [31].

The simulated visual magnitude and constraint violations are shown for this configuration in Fig. 15. For this specific setup, the lunar exclusion angle constraint is always violated. This is the case for most RSOs in a lunar orbit. To

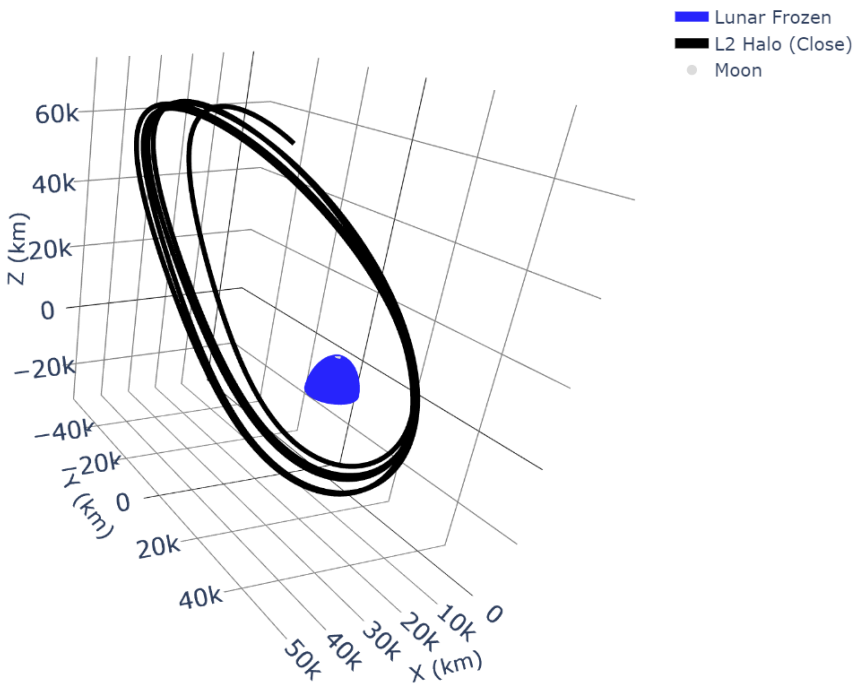

Fig. 14: 3D view of the close L_2 halo observer and lunar frozen orbit RSO in a Moon-centered Earth-Moon rotating frame

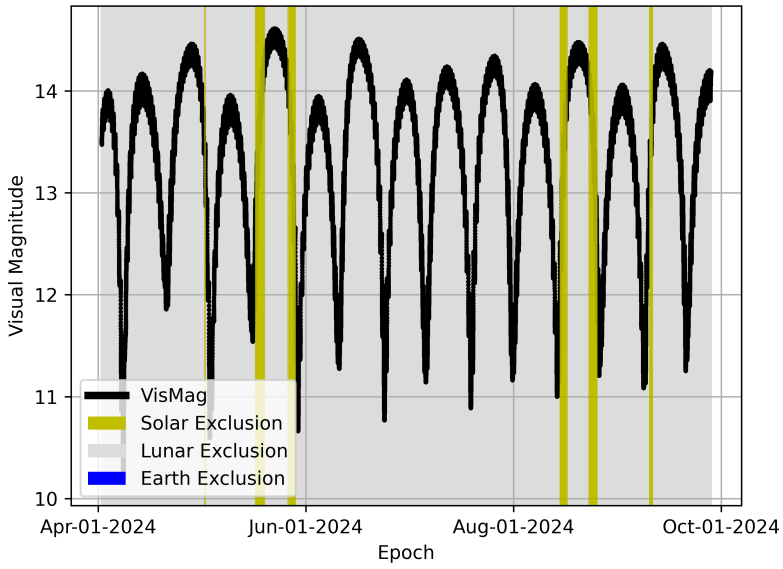

Fig. 15: Simulated visual magnitude of a lunar frozen orbit RSO from an L_2 observer

gather observations in the visual band without violating this constraint, it is most likely required to have an observer in a lunar orbit itself, or a surface asset.

However, to demonstrate what could be possible with certain technological advances, a set of cases were run where

the lunar exclusion angle constraint was significantly decreased. Instead of a full 10 degrees, the constraint was only applied if the RSO was between the observer and the disc of the Moon. The rest of the constraints are still applied as before. This could represent an observer with some sort of optical shield or perhaps an observer gathering measurements in an infrared band, where a spacecraft would likely still reflect sunlight, but the Moon would reflect significantly less than in the visual band.

The filter covariances for this setup with the modified lunar exclusion constraint are shown in Fig. 16.

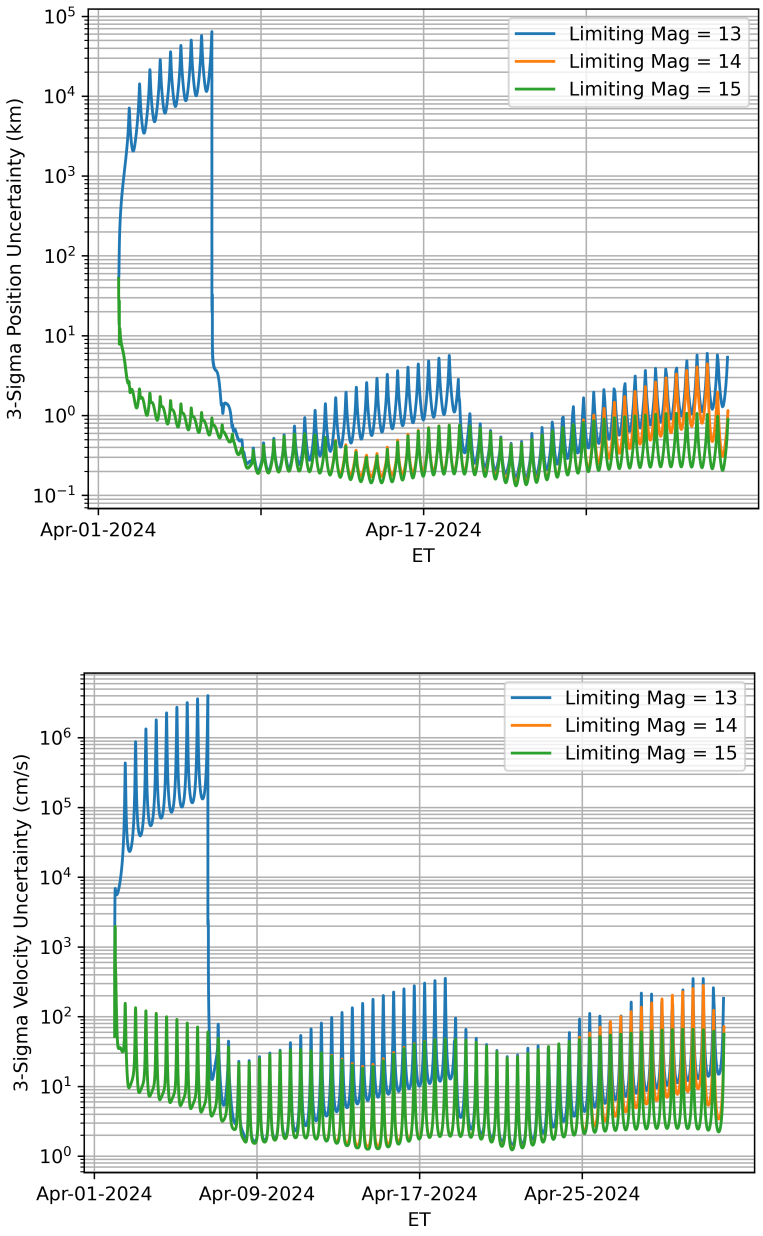

Fig. 16: 3-sigma covariances on the state estimation of a lunar frozen orbit RSO from an L_2 observer

These results show that the most capable optical systems (M = 15) can generate solutions with 3-sigma covariances less than 1 km in position and 2 cm/s in velocity near apolune, and tens of cm/s near perilune. There are short-period oscillations associated with the orbit of the target RSO and longer period oscillations associated with the range between

the observer and RSO.

Note that the large initial increase in covariance on the M = 13 case is caused by there being no measurements for the first few days after the data arc starts. In this particular scenario, the visual magnitude started at around 13.5, so there were no measurements possible until it dropped below 13.

In contrast to the earlier cases, which were estimating the state of a distant L_2 halo orbit, this case did not see any sign of filter divergence, even with large data arcs. With a data arc of approximately 30 days, the filter still produced accurate solutions when compared to the truth. As briefly discussed in Section 4.3, there are studies in dynamical systems theory that have shown that pairs of satellites, one in a lunar orbit and one in a libration point orbit, can provide accurate co-estimation capabilities if there are radiometric measurements between them. In this case, co-estimation was not performed, but this does demonstrate that if lunar exclusion challenges can be overcome, angles-only measurements from a libration point observer to a lunar frozen orbit RSO can provide accurate solutions.

6. CONCLUSIONS AND FUTURE WORK

This analysis has demonstrated angles-only orbit determination between spacecraft in cislunar space, with a particular focus on the Earth-Moon L_2 region. Angles-only orbit determination of RSOs in one particular L_2 halo orbit was found to be a very sensitive problem for multiple space-based cislunar observers, and the designed navigation filters would regularly diverge after 1.5 - 2 revolutions (21 - 28 days). However, for shorter data arcs, the state of the RSO could be estimated to less than 1 km and 1 cm/s from other L_2 halo orbits, and to within 2-3 km and 1-2 cm/s from a large L_2 Lyapunov orbit. If lunar exclusion angles can be overcome such that observations are possible anywhere outside the lunar disc, the tracking of an RSO in a lunar frozen orbit from an L_2 halo was also demonstrated. Each analysis was performed with a number of limiting magnitude cutoffs to study the sensitivity of this observer property on the quality of the estimated solution.

An L_2 Lyapunov orbit with a 1:1 synodic resonance, if properly phased, can provide sunlit observations in large volumes of space near L_2 nearly continuously. However, in this analysis, the greater distance from the RSO to the large Lyapunov orbit resulted in less accurate solutions when compared to the solutions generated by measurements from an NRHO or another standard L_2 halo. Given that an L_2 Lyapunov orbit fully circumnavigates the L_2 Lagrange point (while halo orbits only gather measurements from one side), it is possible that the performance of the Lyapunov observer would improve with longer data arcs.

Future work in this area will seek to improve the stability of the navigation filters and allow for longer data arcs. These longer data arcs could allow for long-term studies of space-based cislunar orbit determination, which could identify seasonal trends based on the Sun-Earth-Moon geometry. A potential method for this could be to utilize a "boxcar" method, where the data arc is continuously shifted forward over time such that it is never longer than 14-21 days. In conjunction with these stability improvements, the authors intend to develop strategies for identifying and estimating stationkeeping maneuvers when they occur. Most libration point orbits, including L_2 halos, require small but somewhat frequent stationkeeping maneuvers to maintain their trajectory. For a cooperative spacecraft, it can be relatively straightforward to estimate maneuvers within a filter, but for a non-cooperative one, it is very important to identify and estimate a maneuver quickly, especially in an unstable environment where relatively small maneuvers can lead to large state changes. The optimal control based estimator (OCBE) strategy developed by Lubey and Scheeres and applied to the problem of cislunar SSA by Greaves and Scheeres would likely be a very promising strategy to replicate into an operational filter [32, 28].

Along these same lines, an important set of analyses to be performed is how quickly a cislunar RSO can be re-acquired and re-correlated after it performs a maneuver. For objects in Earth-centered orbits, the effect of maneuvers on observation residuals is very well-understood, and objects can usually be quickly re-correlated after even large maneuvers. However, for cislunar objects, and particularly objects in Lagrange point orbits, the unstable nature of the trajectories can allow for departures in nearly any direction for extremely low delta-v costs. For a staring sensor, this can make re-acquisition difficult, and it can make correlation difficult for an SSA process. These studies should drive sensor design requirements and revisit rate requirements for future cislunar observers.

Another key improvement to the filter should be to consider the effect of the navigation uncertainty of the observer spacecraft on the OD solution. Assuming perfect state knowledge of the observer means that the results presented here can be thought of as a best case scenario with the given measurement statistics. The focus of this analysis was to be as

observer-agnostic as possible, which is why a baseline uncertainty on the observer was not considered. Operationally however, the effect of adding uncertainty on the state of the observer spacecraft would be to raise the floor of the state uncertainties on the estimate of the RSO. Sensitivity studies should be performed to understand the required observer navigation accuracy to still produce accurate space-based OD solutions.

Finally, while incorporating high-fidelity optical modeling was not a goal of this work, implementing some of this modeling could be helpful in increasing the realism of the given simulations. For example, instead of generating measurements with a fixed noise value at a fixed time step, measurements could be generated based on realistic integration times required to provide a necessary SNR, or the noise value could be varied based on the SNR. Adding these improvements departs from the broad strategy of trying to be observer-agnostic, but moves towards a simulation framework that can be utilized to simulate the performance based on hardware specifications for a given CCD and optical telescope.

7. REFERENCES

[1] J. Carrico Jr., J. Carrico III, J. Decoto, A. Ferris, R. Lebois, M. Loucks, T. Mclaughlin, N. Singh, and S. Tilley, "Chang'e 5: Trajectory Resconstruction," in *AAS/AIAA Astrodynamics Specialist Conference*, 2021.

[2] P. Dao, K. Haynes, V. Frey, C. Hufford, K. Schindler, T. Payne, and J. Hollon, "Simulated Photometry of Objects in Cislunar Orbits," in *Advanced Maui Optical and Space Surveillance Technologies Conference (AMOS)*, 2020.

[3] M. R. Ackermann, R. R. Riziah, P. C. Zimmer, J. T. McGraw, and D. D. Cox, "A Systematic Examination of Ground-Based and Space-Based Approaches to Optical Detection and Tracking of Satellites," in *31st Space Symposium*, 2015.

[4] M. Bolden, T. Craychee, and E. Griggs, "An Evaluation of Observing Constellation Orbit Stability, Low Signal-to-Noise, and the Too-Short-Arc Challenges in the Cislunar Domain," in *Advanced Maui Optical and Space Surveillance Technologies Conference (AMOS)*, 2020.

[5] M. J. Holzinger, C. C. Chow, and P. Garretson, "A Primer on Cislunar Space," tech. rep., Air Force Research Laboratory, 2021.

[6] S. Knister, B. R. Williams, D. Hayhurst, K. W. John, and B. D. Little, "Evaluation Framework for Cislunar Space Domain Awareness Systems," in *AIAA/AAS Astrodynamics Specialist Conference*, 2021.

[7] P. M. Cunio, M. J. Bever, and B. R. Flewelling, "Payload and Constellation Design for a Solar Exclusion-Avoiding Cislunar SSA Fleet," in *Advanced Maui Optical and Space Surveillance Technologies Conference (AMOS)*, 2020.

[8] J. K. Vendl and M. J. Holzinger, "Cislunar Periodic Orbit Analysis for Persistent Space Object Detection Capability," in *AAS/AIAA Astrodynamics Specialist Conference*, 2020.

[9] E. E. Fowler, S. B. Hurtt, and D. A. Paley, "Observability Metrics for Space-Based Cislunar Domain Awareness," in *AAS/AIAA Astrodynamics Specialist Conference*, 2020.

[10] C. Frueh, K. Howell, K. Demars, S. Bhadauria, and M. Gupta, "Cislunar Space Traffic Management: Surveillance Through Earth-Moon Resonance Orbits," in *8th European Conference on Space Debris*, (Darmstadt, Germany), ESA Space Debris Office, 2021.

[11] M. Gupta, K. C. Howell, and C. Frueh, "Earth-Moon Multi-Body Orbit to Facilitate Cislunar Surveillance Activities," in *AIAA/AAS Astrodynamics Specialist Conference*, 2021.

[12] J. Williams, D. E. Lee, R. J. Whitley, K. A. Bokelmann, D. C. Davis, and C. F. Berry, "Targeting Cislunar Near Rectilinear Halo Orbits for Human Space Exploration," *Advances in the Astronautical Sciences*, vol. 160, pp. 3125–3144, 2017.

[13] E. W. Kayser, J. S. Parker, M. Bolliger, T. Gardner, and B. Cheetham, "The Cislunar Autonomous Positioning System Technology Operations and Navigation Experiment (CAPSTONE)," in *AAS/AIAA Astrodynamics Specialist Conference*, 2020.

[14] M. Hejduk, "Specular and Diffuse Components in Spherical Satellite Photometric Modeling," in *Advanced Maui Optical and Space Surveillance Technologies Conference (AMOS)*, 2011.

[15] J. Smith, T. Drain, S. Bhaskaran, and T. J. Martin-Mur, "MONTE for Orbit Determination," in *International Symposium on Space Flight Dynamics*, 2017.

[16] S. Evans, W. Taber, T. Drain, J. Smith, H.-C. Wu, M. Guevara, R. Sunseri, and J. Evans, "MONTE: The Next Generation of Mission Design and Navigation Software," *CEAS Space Journal*, vol. 10, 2018.

[17] M. R. Thompson, E. Kayser, J. S. Parker, C. Ott, T. Gardner, and B. W. Cheetham, "Navigation Design of the

CAPSTONE Mission Near NRHO Insertion," in *AAS/AIAA Astrodynamics Specialist Conference*, 2021.
[18] N. L. Parrish, M. J. Bolliger, E. Kayser, M. R. Thompson, J. S. Parker, B. W. Cheetham, D. C. Davis, and D. J. Sweeny, "Near Rectilinear Halo Orbit Determination with Simulated DSN Observations," in *AIAA SciTech 2020 Forum*, (Orlando, FL), 2020.
[19] M. Bolliger, M. R. Thompson, N. P. Ré, C. Ott, and D. C. Davis, "Ground-Based Navigation Trades for Operations in Gateway's Near Rectilinear Halo Orbit," in *31st AAS/AIAA Space Flight Mechanics Meeting*, 2021.
[20] K. A. Hill, *Autonomous Navigation in Libration Point Orbits*. PhD thesis, University of Colorado, 2007.
[21] K. Hill and G. H. Born, "Autonomous Interplanetary Orbit Determination Using Satellite-to-Satellite Tracking," *Journal of Guidance, Control, and Dynamics*, vol. 30, no. 3, pp. 679–686, 2007.
[22] R. Leitch and I. Hemphill, "Sapphire: A Small Satellite System for the Surveillance of Space," in *Small Satellite Conference*, 2010.
[23] A. Scott, J. Hackett, and K. Man, "On-Orbit Results for Canada's Sapphire Optical Payload Alan Scott Kam Man," in *Advanced Maui Optical and Space Surveillance Technologies Conference (AMOS)*, 2013.
[24] P. Maskell and L. Oram, "Sapphire: Canada's Answer to Space-Based Surveillance of Orbital Objects," in *Advanced Maui Optical and Space Surveillance Technologies Conference (AMOS)*, 2008.
[25] D. A. Vallado, M. Ackermann, P. Cefola, and R. Kiziah, "Orbital Strategies to Mitigate the Solar Exclusion Effect on Space-Based Observation of the Geosynchronous Belt," in *AIAA/AAS Astrodynamics Specialist Conference, 2016*, 2016.
[26] T. Gardner, B. Cheetham, A. Forsman, C. Meek, E. Kayser, J. Parker, M. Thompson, T. Latchu, R. Rogers, B. Bryant, and T. Svitek, "CAPSTONE : A CubeSat Pathfinder for the Lunar Gateway Ecosystem," in *Small Satellite Conference*, 2021.
[27] D. C. Davis, F. Khoury, K. C. Howell, and D. J. Sweeny, "Phase Control and Eclipse Avoiding in Near Rectilinear Halo Orbits," in *43rd AAS Guidance, Navigation, and Control Conference*, (Breckenridge, Colorado), 2020.
[28] J. Greaves and D. Scheeres, "Maneuver Detection for Cislunar Vehicles Using Optical Measurements," in *Advanced Maui Optical and Space Surveillance Technologies Conference (AMOS)*, 2020.
[29] T. A. Ely, "Stable Constellations of Frozen Elliptical Inclined Lunar Orbits," *Journal of the Astronautical Sciences*, vol. 53, no. 3, pp. 301–316, 2005.
[30] T. Nie and P. Gurfil, "Lunar Frozen Orbits Revisited," *Celestial Mechanics and Dynamical Astronomy*, vol. 130, no. 10, 2018.
[31] L. Zhang, "Development and Prospect of Chinese Lunar Relay Communication Satellite," *Space: Science & Technology*, vol. 2021, 2021.
[32] D. P. Lubey and D. J. Scheeres, "An Optimal Control Based Estimator for Maneuver and Natural Dynamics Reconstruction," in *Advanced Maui Optical and Space Surveillance Technologies Conference (AMOS)*, 2013.